Sustained Release of Calcium Elicited by Membrane Depolarization in Ryanodine-Injected Mouse Skeletal Muscle Fibers

Claude Collet and Vincent Jacquemond
Laboratoire de Physiologie des Eléments Excitables, Université Claude Bernard Lyon 1, F69622 Villeurbanne, France

ABSTRACT The effect of micromolar intracellular levels of ryanodine was tested on the myoplasmic free calcium concentration ($[Ca^{2+}]_i$) measured from a portion of isolated mouse skeletal muscle fibers voltage-clamped at −80 mV. When ryanodine-injected fibers were transiently depolarized to 0 mV, the early decay phase of $[Ca^{2+}]_i$ upon membrane repolarization was followed by a steady elevated $[Ca^{2+}]_i$ level. This effect could be qualitatively well simulated, assuming that ryanodine binds to release channels that open during depolarization and that ryanodine-bound channels do not close upon repolarization. The amplitude of the postpulse $[Ca^{2+}]_i$ elevation depended on the duration of the depolarization, being hardly detectable for pulses shorter than 100 ms, and very prominent for duration pulses of seconds. Within a series of consecutive pulses of the same duration, the effect of ryanodine produced a staircase increase in resting $[Ca^{2+}]_i$, the slope of which was approximately twice larger for depolarizations to 0 or +10 mV than to −30 or −20 mV. Overall results are consistent with the "open-locked" state because of ryanodine binding to calcium release channels that open during depolarization. Within the voltage-sensitive range of calcium release, increasing either the amplitude or the duration of the depolarization seems to enhance the fraction of release channels accessible to ryanodine.

INTRODUCTION

In skeletal muscle, excitation-contraction (E-C) coupling results from opening of sarcoplasmic reticulum (SR) calcium release channels that are under the control of the voltage sensors present in the adjacent transverse tubule membrane. The present understanding of the mechanisms involved in the control of SR calcium release has greatly benefited from the use of various pharmacological tools that specifically bind to the release channels and modulate their operating mode. In this respect, the neutral plant alkaloid ryanodine has been widely used as a functional probe of the release channel (Sutko et al., 1997). Ryanodine has complex effects on muscle contractile activity; it was reported to depress twitch and tetanic tension, and to induce a slowly developing contracture (Fryer et al., 1989). The detailed effects of the interaction of ryanodine with the release channel have been most extensively studied using single-channel recordings, isolated SR vesicles, and skinned fibers (Meissner, 1986; Lattanzio et al., 1987; Rousseau et al., 1987; Su, 1987; Bull et al., 1989; Lamb and Stephenson, 1990; Buck et al., 1992; Meissner and el-Hashem, 1992). Ryanodine displays both high-affinity and low-affinity binding sites on the calcium release channel complex. At low concentrations (<10 μM), it is generally believed to lock the channel into a partially open state in which it is no longer sensitive to different modulators that normally affect its activity (Meissner and el-Hashem, 1992). This open-state stabilization was also recently confirmed in permeabilized frog skeletal muscle fibers by the observation of ryanodine-induced, long-lasting, local calcium events (Gonzalez et al., 2000). Conversely, data concerning the effect of ryanodine on the regulation of global intracellular Ca^{2+} concentration in isolated skeletal muscle fibers under voltage control are limited. Mainly, this issue was addressed by Garcia et al. (1991) in frog fibers under conditions that did not allow measurement of the resting $[Ca^{2+}]_i$ level, and to our knowledge, there has been no equivalent study performed on mammalian muscle fibers. This problem is of importance as a full understanding of the mechanism of action of ryanodine should require integration of detailed results from both disrupted and intact preparations. For instance, there has been so far no clear evidence given for functional consequences of the "open lock" phenomenon from $[Ca^{2+}]_i$ measurements in voltage-clamped mammalian fibers. As a consequence, it is also not clear whether or not ryanodine-bound channels are still under the control of the voltage sensor in these conditions. In the present study, we examined the effect of intracellularly applied ryanodine on the resting $[Ca^{2+}]_i$ level and on the changes in $[Ca^{2+}]_i$ elicited by voltage-clamp depolarizations in isolated mouse skeletal muscle fibers. Our main goal was to characterize how calcium release is affected by the presence of the alkaloid in an intact mammalian skeletal muscle fiber. In addition, because ryanodine should essentially bind to release channels that are in an open state, investigation of the parameters and conditions that modulate its effects was expected to enlighten physiologically relevant aspects of the control of calcium release.

Submitted August 6, 2001, and accepted for publication November 27, 2001.

Address reprint requests to Vincent Jacquemond, Laboratoire de Physiologie des Eléments Excitables, Université Claude Bernard-Lyon 1, ERS CNRS 2019, Bât. 401 B, 43 Boulevard du 11 Novembre 1918, F69622 Villeurbanne Cedex, France. Tel.: 33-4-72-43-10-32; Fax: 33-4-78-94-68-20; E-mail: vincent.jacquemond@univ-lyon1.fr.

0006-3495/02/03/1509/15 $2.00

MATERIALS AND METHODS

Preparation of the muscle fibers

Experiments were performed on single skeletal fibers isolated from the flexor digitorum brevis muscles from adult mice. All experiments were performed in accordance with the guidelines of the French Ministry of Agriculture (87/848) and of the European Community (86/609/EEC). Details of procedures for enzymatic isolation of single fibers, partial insulation of the fibers with silicone grease, and intracellular dye loading were as described previously (Jacquemond, 1997; Collet et al., 1999). In brief, mice were killed by cervical dislocation after halothane anesthesia. Muscles were removed and treated with collagenase (Sigma type 1, Sigma-Aldrich, Saint Quentin Fallavier, France) for 60–75 min at 37°C in presence of tyrode as external solution. Single fibers were then obtained by triturating the muscles within the experimental chamber. The full length and diameter of the fibers typically ranged within 500–700 μm and 40–60 μm, respectively. The major part of a single fiber was electrically insulated with silicone grease so that whole-cell voltage clamp could be achieved on a short portion (60–120 μm long) of the fiber extremity. Before patch clamp, indo-1 was introduced locally into the fiber end by pressure microinjection through a separate micropipette containing 0.5 mM indo-1 dissolved in an intracellular-like solution containing (in mM) 120 K-glutamate, 5 Na_2-ATP, 5 Na_2-phosphocreatine, 5.5 $MgCl_2$, 5 glucose, 5 HEPES adjusted to pH 7.2 with K-OH. For ryanodine-injected fibers, the alkaloid was added at either 0.1 or 0.8 mM to the injected solution. Although we could not precisely estimate the amount of fiber volume that was injected, this procedure was expected to achieve final intracellular ryanodine concentrations in the tens of micromolar and hundreds of micromolar range, respectively (Csernoch et al., 1998 for details concerning microinjections). Microinjections were carried out with the pipette tip inserted through the silicone within the insulated part of the fiber. After being microinjected, fibers were left for ~1 h to allow for dye (and ryanodine) intracellular equilibration. All experiments were performed at room temperature (20–22°C), in the presence of an extracellular solution containing (in mM) 140 TEA-methanesulfonate, 2.5 $CaCl_2$, 2 $MgCl_2$, 10 TEA-HEPES, and 0.002 tetrodotoxin, pH 7.20.

Electrophysiology

An RK-400 patch-clamp amplifier (Bio-Logic, Claix, France) was used in whole-cell configuration. Command voltage-pulses generation and data acquisition were performed using commercial software (Biopatch Acquire, Bio-Logic) driving an analog/digital, digital/analog converter (Lab Master DMA board, Scientific Solutions Inc., Solon, OH). Analog compensation was systematically used to decrease the effective series resistance. Voltage-clamp was performed with a microelectrode filled with the intracellular-like solution. The tip of the microelectrode was inserted through the silicone, within the insulated part of the fiber. Membrane depolarizations were applied every 30 s from a holding command potential of −80 mV.

Fluorescence measurements

The optical set-up for indo-1 fluorescence measurements was described previously (Jacquemond, 1997). In brief, a Nikon Diaphot epifluorescence microscope (Nikon Corporation, Tokyo, Japan) was used in diafluorescence mode. For indo-1 excitation, the beam of light from a high-pressure mercury bulb set on top of the microscope was passed through a 335-nm interference filter and focused onto the preparation using a quartz aspherical doublet. The emitted fluorescence light was collected by a 40× objective and simultaneously detected at 405 ± 5 nm (F_{405}) and 470 ± 5 nm (F_{470}) by two photomultipliers. The fluorescence measurement field was 40 μm in diameter and the silicone-free extremity of each tested fiber was placed in the middle of the field. Background fluorescence at both emission wavelengths was measured next to each tested fiber and was then subtracted from all measurements. On each fiber, a fluorescence measurement was taken before impaling the fiber with the microelectrode used for voltage-clamp. These data were used to determine what is referred to as the initial, resting, free calcium concentration. The presence of movement artifacts was routinely detected in the raw indo-1 fluorescence transients measured in response to strong membrane depolarizations. As described by Jacquemond (1997), this could be assessed from nonlinearity between the normalized time course of change in fluorescence at the two wavelengths. In most cases, however, the motion-related changes in fluorescence were of small amplitude as compared with the calcium-dependent changes in fluorescence. Furthermore, even when clearly present in the original fluorescence traces, motion artifacts seemed to be largely eliminated in the ratio (F_{405}/F_{470}) signal.

Calibration of the indo-1 response and $[Ca^{2+}]_i$ calculation

Free calcium concentration was calculated using the standard ratio method with the parameters: $R = F_{405}/F_{470}$, and R_{min}, R_{max}, K_D, β having their usual definition. No correction was made for indo-1-Ca^{2+} binding and dissociation kinetics, so that the derived time course of change in $[Ca^{2+}]_i$ does not exactly reflect the true amplitude and time course of change in ionized calcium. A series of in vitro calibrations was performed on the experimental set-up using glass capillary tubes filled with solutions containing various concentrations of free calcium prepared as described previously (Jacquemond, 1997), except that the pH of all solutions was set to 7.25 instead of 7.00. In one set of calibrations, solutions also contained 50 μM indo-1, whereas in another set, solutions contained 50 μM indo-1 and 100 μM ryanodine. Results showed that the value for indo-1 K_D, as well as for R_{min} and R_{max}, were essentially unaffected in the presence of ryanodine. Values for R_{min}, R_{max}, and K_D, were 0.38, 2.13, and 310 nM in control, and 0.37, 2.16, and 280 nM in the presence of ryanodine (not illustrated). A common value of 300 nM was used for the indo-1 K_D in all $[Ca^{2+}]$ calculations. In vivo values for R_{min}, R_{max}, and β were measured using procedures described by Collet et al. (1999). Results were either expressed in terms of indo-1 percentage of saturation or in actual free calcium concentration (Jacquemond, 1997; Csernoch et al., 1998).

Simulation of $[Ca^{2+}]_i$ transients and calculation of intrinsic buffers occupancy

The procedure described by Timmer et al. (1998) was used to simulate $[Ca^{2+}]_i$ transients elicited by membrane depolarization. A defined Ca^{2+} release rate waveform was used as input flux in a simple calcium distribution model that reproduced the basic features of Ca^{2+} regulation in a muscle cell. In brief, synthetic Ca^{2+} release rate records were generated as described by Timmer et al. (1998). The Ca^{2+} flux waveform included an early peak that preceded a steady level, as there is a massive body of evidence for such a time course to underlie the change in $[Ca^{2+}]_i$ produced by a step voltage-clamp depolarization in frog (Rios and Pizarro, 1991) as well as in mammalian skeletal muscle (Garcia and Schneider, 1993; Shirokova et al., 1996; Szentesi et al., 1997). A small, time-independent Ca^{2+} "leak" flux was also included in the synthetic release records. Two sets of calculations were performed. In one set we used the same calcium distribution model as Timmer et al. (1998), including a saturable slow compartment CaS (total sites concentration S_{total} = 100 μM, "on" rate constant $k_{on,CaS}$ = 0.01 $\mu M^{-1}\cdot ms^{-1}$, "off" rate constant $k_{off,CaS}$ = 0.0003 ms^{-1}), a nonsaturable calcium uptake (rate constant k_{ns} = 0.4 ms^{-1}), and an instantaneously equilibrating nonsaturating compartment the occupancy of which was assumed to be equal to 30 times the $[Ca^{2+}]_i$. In another set of calculations we used a more elaborate model that took into account the presumed properties of the main calcium buffering and uptake mechanisms commonly believed to operate in skeletal muscle, using values from the

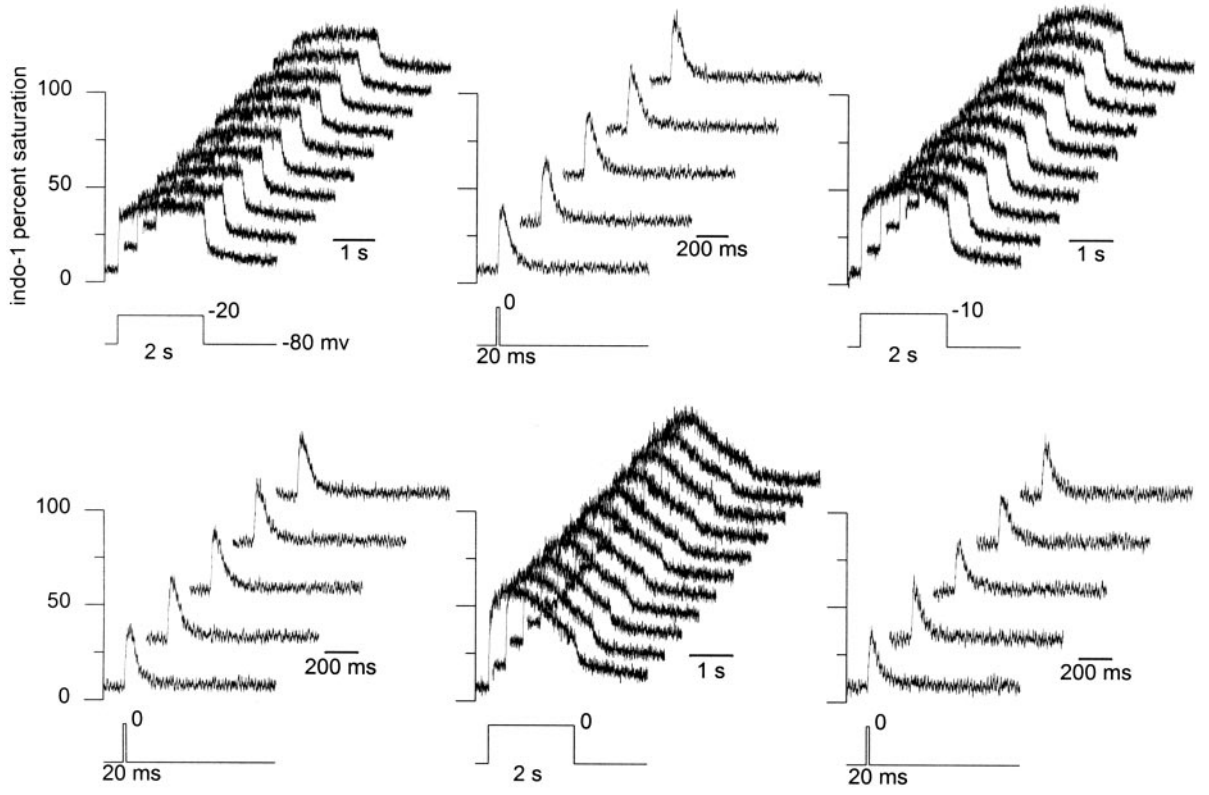

FIGURE 1 Stability of $[Ca^{2+}]_i$ measurements over long periods of time under the silicone-clamp conditions. Indo-1 saturation traces recorded from a same fiber in response to depolarizations of various amplitude and duration. In each panel, traces were obtained in response to the pulse shown underneath, that was applied several times; traces are presented with an *x* and *y* offset for clarity.

literature for the parameters. This model included troponin C binding sites with a total sites concentration TN_{total} of 250 μM, an on rate constant $k_{on,CaTN}$ of 0.0575 $\mu M^{-1}\cdot ms^{-1}$ and an off rate constant $k_{off,CaTN}$ of 0.115 ms^{-1} (Baylor et al., 1983); Ca-Mg binding sites on parvalbumin with a total sites concentration PV_{total} = 700 μM (Garcia and Schneider, 1993), on rate constant for Ca^{2+} $k_{on,CaPV}$ = 0.125 $\mu M^{-1}\cdot ms^{-1}$, off rate constant for Ca^{2+} $k_{off,CaPV} = 5.10^{-4}$ ms^{-1}, on rate constant for Mg^{2+} $k_{on,MgPV} = 3.3.10^{-5}$ $\mu M^{-1}\cdot ms^{-1}$, off rate constant for Mg^{2+} $k_{off,MgPV} = 3.10^{-3}$ ms^{-1} (Baylor et al., 1983). The rate of calcium transport across the SR membrane was considered to be proportional to the fractional occupancy of the SR pump sites by calcium with a dissociation constant $Kd\ Ca_{pump}$ of 2 μM and a maximum pump rate of 1 $\mu M\cdot ms^{-1}$. The resting $[Ca^{2+}]_i$ was assumed to be 0.1 μM. Equilibrium dissociation constants obtained from the ratio of the corresponding values of the off and on rate constants were used to calculate the initial resting calcium occupancy of the buffers. For parvalbumin, the initial $[Mg^{2+}]$ was assumed to be 1.5 mM (Csernoch et al., 1998), and was used together with the resting $[Ca^{2+}]_i$ value of 0.1 μM to calculate the initial calcium and magnesium occupancy of parvalbumin. Under these conditions, the fractional calcium and magnesium occupancy of parvalbumin is 59% and 39%, respectively.

Statistics

Least-squares fits were performed using a Marquardt-Levenberg algorithm routine included in Microcal Origin (Microcal Software Inc., Northampton, MA). Data values are presented as means ± SE for *n* fibers, where *n* is specified in Results. Statistical significance was determined using a Student's *t* test assuming significance for $P < 0.05$.

RESULTS

Stability of the depolarization-induced $[Ca^{2+}]_i$ transients under control conditions

Fig. 1 shows a series of indo-1 percentage saturation records obtained from the same muscle fiber in response to successive depolarizations of various amplitudes and durations. Each depolarization was repeated several times at a frequency of 0.033 Hz. The transients obtained in response to each series of a same depolarization are shown with an *x* and *y* offset within the same panel of Figure 1, respectively. Overall results clearly illustrate the fact that our experimental conditions allow the possibility of achieving quite stable $[Ca^{2+}]_i$ transients recordings over long periods of time, even when fibers were challenged by many depolarizing pulses of seconds duration. In that particular example, the fiber was successively depolarized by series of pulses of 2-s duration to −20 mV, 20-ms duration to 0 mV, 2-s duration to −10 mV, 20-ms duration to 0 mV, and 2-s duration to 0 mV, and 20-ms duration to 0 mV, respectively. Measurements were taken over a period of time of ~1 h, during which resting $[Ca^{2+}]_i$, as estimated from the baseline level of indo-1 saturation, increased from ~20 to 40 nM between the first and last depolarization. In response to 2-s duration pulses to values more positive than −10 mV, the indo-1 signals were routinely

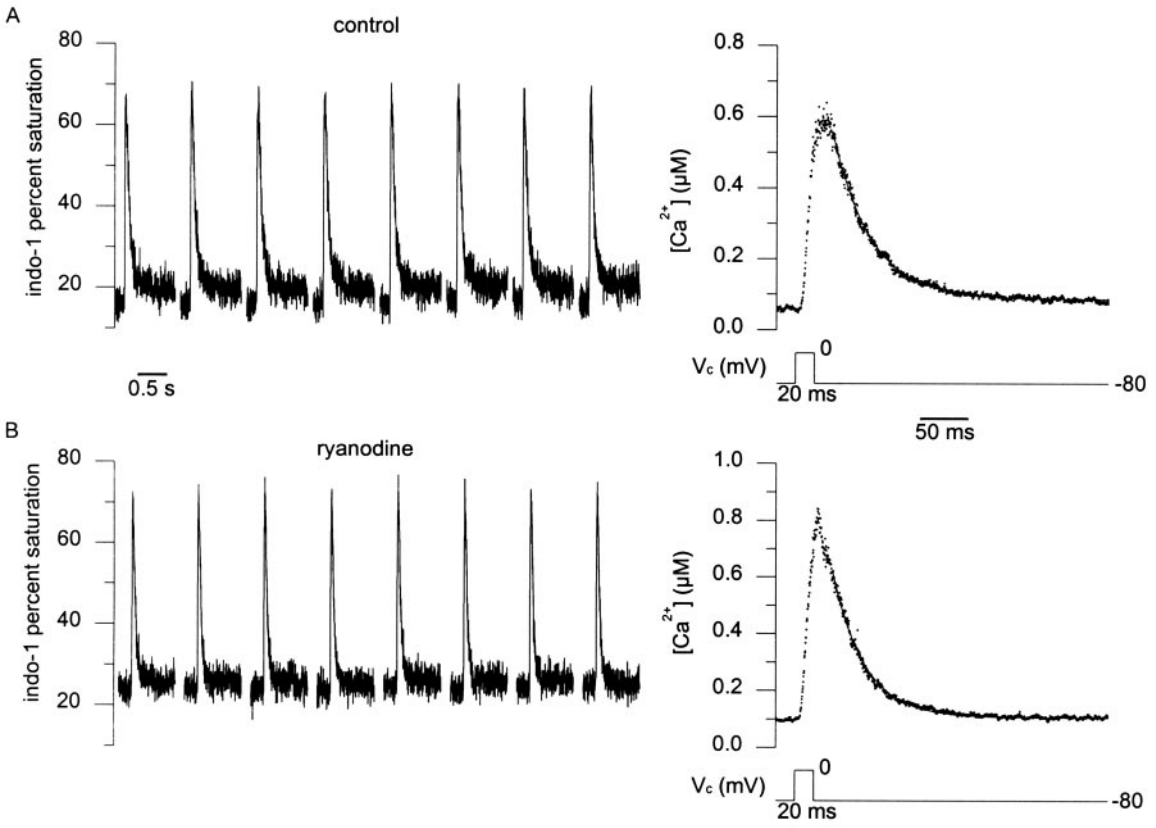

FIGURE 2 $[Ca^{2+}]_i$ transients elicited by short depolarizations in a control (*A*) and in a ryanodine-injected fiber (*B*). Indo-1 saturation signals (left) and corresponding mean $[Ca^{2+}]_i$ transient (right) obtained in response to a 20-ms depolarizing pulse to 0 mV applied every 30 s in a control (*A*) and in a ryanodine-injected fiber (*B*). The smooth curve superimposed to the decay of the $[Ca^{2+}]_i$ traces corresponds to the result from fitting a single exponential plus constant function. Values for the time constant of decay were 43 ms (*A*) and 33 ms (*B*).

observed to spontaneously decay during the pulse, as previously reported in other studies (Brum et al., 1988).

Initial resting $[Ca^{2+}]_i$ in control and in ryanodine-injected fibers

As ryanodine was previously reported to potentially induce muscle contracture, we measured the initial resting $[Ca^{2+}]_i$ level in control and in ryanodine-injected fibers before any membrane depolarization was applied. Under our conditions, resting $[Ca^{2+}]_i$ was 89 ± 12 nM ($n = 36$) and 93 ± 7 nM ($n = 32$) in control and in ryanodine-injected fibers, respectively, indicating that the consequences of any putative spontaneous ryanodine-induced Ca^{2+} release remained undetectable under the present conditions.

Effect of ryanodine on $[Ca^{2+}]_i$ transients elicited by short (20 ms long) depolarizing pulses

Fig. 2 shows indo-1 Ca^{2+} transients elicited by short depolarizing pulses in a control fiber (Fig. 2 *A*) and in a ryanodine-injected fiber (Fig. 2 *B*). Transients were elicited by a 20-ms long depolarization to 0 mV, applied every 30 s. Under our conditions, such short pulses are routinely used because they usually elicit $[Ca^{2+}]_i$ transients of relatively low maximal amplitude which do not produce prolonged heavy levels of dye saturation. In Fig. 2, *A* and *B*, the left panel shows the successive indo-1 percentage saturation traces, whereas the right panel shows the corresponding mean $[Ca^{2+}]_i$ transient. There was no obvious qualitative difference between the Ca^{2+} transients in the control and in the ryanodine-injected fiber; both were fairly stable, peaked within the submicromolar range, and decayed rapidly upon repolarization. In Fig. 2, the result from fitting a single exponential plus constant function to the decaying phase of the mean calcium transient from the control and from the ryanodine-injected fiber is shown as a superimposed solid curve. The time constant of $[Ca^{2+}]_i$ decay was 43 ms and 33 ms in the control and in the ryanodine-injected fiber, respectively.

Fig. 3 shows the mean values for the resting $[Ca^{2+}]_i$ (*A*), peak change in $[Ca^{2+}]_i$ (*B*), time constant of $[Ca^{2+}]_i$ decay (*C*), and final $[Ca^{2+}]_i$ level (*D*) from the first and last transient measured in control and in ryanodine-injected fibers to which the protocol shown in Fig. 2 was applied.

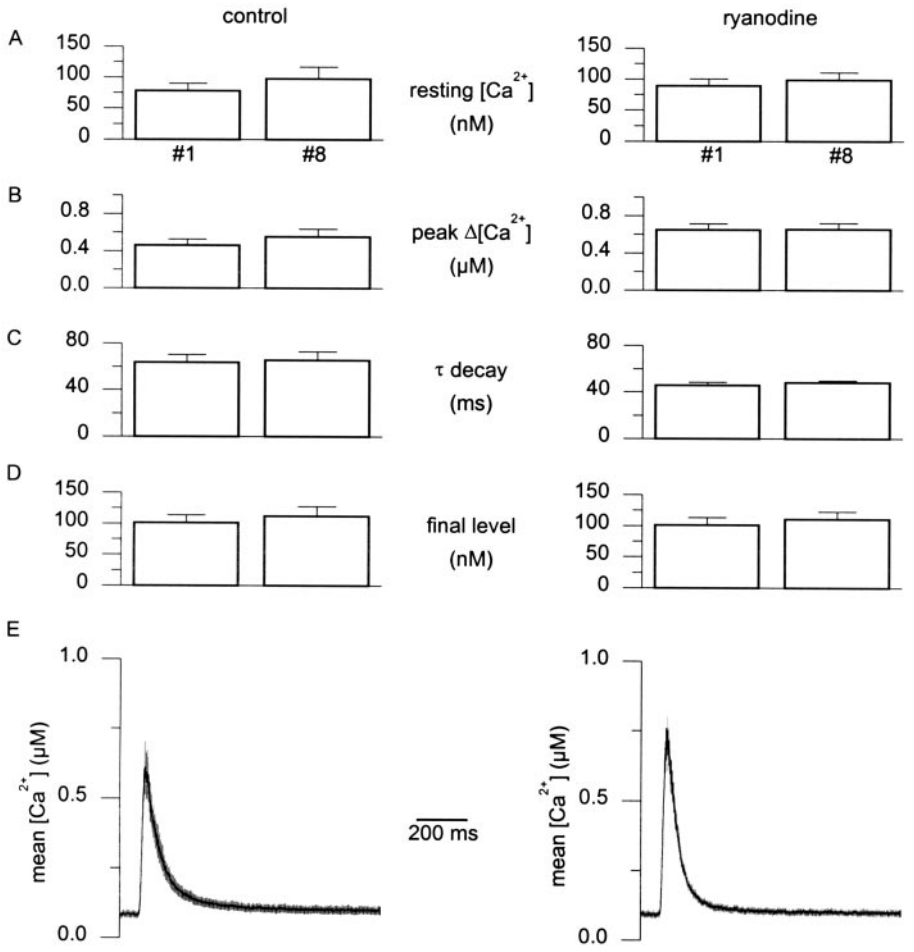

FIGURE 3 Average properties of $[Ca^{2+}]_i$ transients elicited by short depolarizing pulses in control and in ryanodine-injected fibers. Data were obtained from 14 control fibers (left) and 10 ryanodine-injected fibers (right) that were stimulated by a series of eight successive 20-ms depolarizations to 0 mV (same protocol as in Fig. 1). Mean ± SE values for resting $[Ca^{2+}]_i$ (*A*); peak $\Delta[Ca^{2+}]_i$ (*B*); time constant of $[Ca^{2+}]_i$ decay (*C*); and final $[Ca^{2+}]_i$ level (*D*) corresponding to the transients measured in response to the first (1) and last pulse (8) that was applied. (*E*), Overall mean (*continuous trace*) ± SE (*shaded area*) $[Ca^{2+}]_i$ trace elicited by 20-ms pulses to 0 mV in control fibers (left, $n = 14$) and in ryanodine-injected fibers (right, $n = 10$).

There was no significant difference in the values for all parameters between the first and last transient of the series, indicating no systematic differential evolution of the preparation under the two conditions. However, when comparing the mean values for all parameters between the two conditions, the time constant of $[Ca^{2+}]_i$ decay was found to be significantly decreased in the ryanodine-injected fibers as compared with the control ones, whereas other parameters were not statistically different. The mean time constant of $[Ca^{2+}]_i$ decay after the first depolarization was 64 ± 7 ms ($n = 14$) and 46 ± 3 ms ($n = 10$) in control and in ryanodine-injected fibers, respectively. The mean $[Ca^{2+}]_i$ transient from all control and ryanodine-injected fibers that took the eight successive 20-ms depolarizations to 0 mV were averaged. In Fig. 3 *E*, the graphs show the corresponding mean (± SE) $[Ca^{2+}]_i$ versus time in the two conditions, qualitatively illustrating the basic features of the $[Ca^{2+}]_i$ transients from that series of measurements.

Increasing the duration of the depolarizing pulses reveals a clear effect of ryanodine on the post-pulse $[Ca^{2+}]_i$ level

In Fig. 4, panels *B* and *C* show indo-1 percentage saturation traces elicited by depolarizing pulses to 0 mV of increasing duration, in a control fiber and in a ryanodine-injected fiber, respectively. Pulses of 20-, 220-, 420-, and 620-ms duration were successively applied to both fibers (Fig. 4 *A*), and for a given duration, each pulse was repeated four times before its duration was increased. The time interval between two consecutive pulses was always 30 s. In each panel of Fig. 4, *B* and *C*, transients elicited by the four pulses of same duration are shown superimposed. In the control fiber (Fig. 4 *B*), the four transients obtained in response to each series of pulses of identical duration were well reproducible and thus not distinguishable from one another. As shown in the previous section, this also held true for the transients elicited

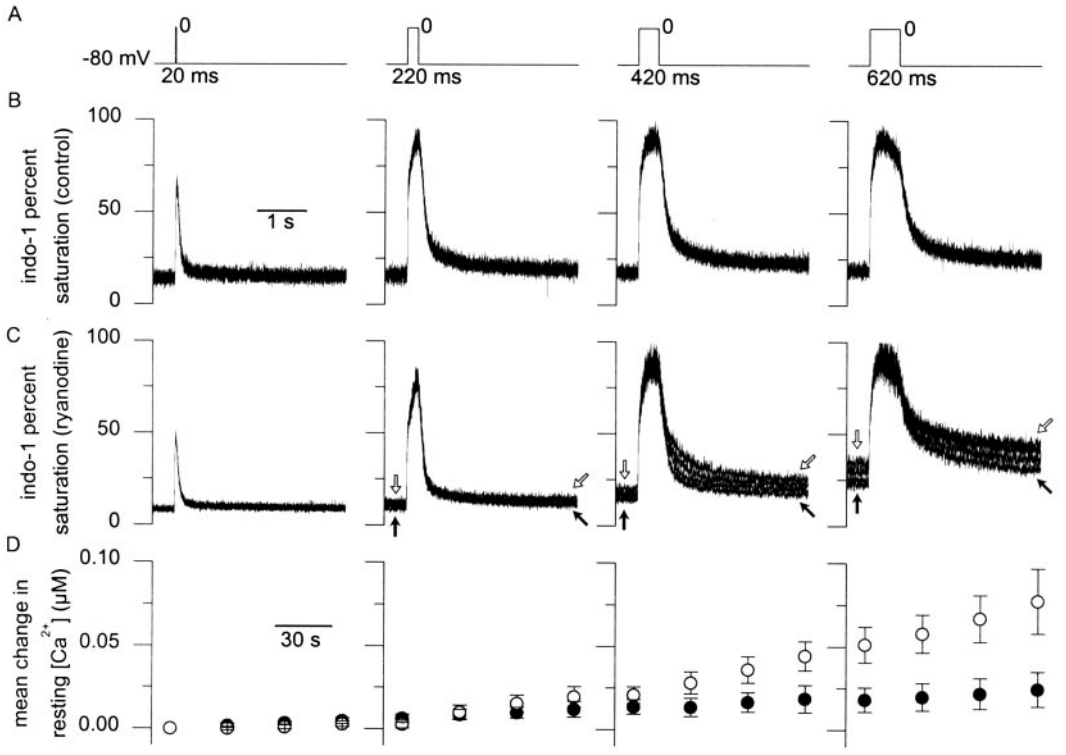

FIGURE 4 $[Ca^{2+}]_i$ signals evoked by depolarizations of increasing duration in control fibers and in ryanodine-injected fibers. (*A*), Pulse protocol: depolarizing pulses of 20, 220, 420, and 620 ms to 0 mV were successively applied. A 30-s time period was allowed between two consecutive pulses. For a given duration, each pulse was repeated four times, and then duration was incremented. (*B* and *C*), Corresponding indo-1 saturation signals in a control fiber and in a ryanodine-injected fiber, respectively; transients elicited by pulses of same duration are shown superimposed. (*C*), Filled arrows point to the initial and final indo-1 saturation level of the transient elicited by the first 220-, 420-, and 620-ms pulse, respectively. Open arrows point to the initial and final indo-1 saturation level of the transient elicited by the fourth 220-, 420-, and 620-ms pulse, respectively. (*D*), Time course of mean (± SE) change in resting $[Ca^{2+}]_i$ in control fibers (●, $n = 5$) and in ryanodine-injected fibers (○, $n = 4$) over the course of the above experimental protocol.

by 20-ms duration pulses in the ryanodine-injected fiber, but not any more for the transients elicited by longer duration pulses. For those, the indo-1 saturation level tended to remain elevated after each pulse, as compared with the corresponding prepulse baseline level. In Fig. 4 *C*, this is indicated by filled and open arrows which point to the pre- and postpulse indo-1 saturation level corresponding to the first and fourth transient that was measured in each series, respectively. The relative amount by which the indo-1 saturation remained elevated after each pulse seemed to be larger as the pulse duration was increased, the effect being barely detectable for the 220-ms duration pulses and much more prominent for the 420- and 620-ms duration pulses. In Fig. 4 *D*, the mean change in resting $[Ca^{2+}]_i$ measured from five control fibers (●) and four ryanodine-injected fibers (○) to which this same protocol was applied, is plotted versus time. In each fiber, the resting $[Ca^{2+}]_i$ was calculated from the baseline indo-1 saturation level preceding each pulse. The value measured before the first (20-ms duration) depolarization was then subtracted from all subsequent measured values. There was a clear tendency for the resting $[Ca^{2+}]_i$ to increase in the ryanodine-injected fibers, although on average, as compared with the control fibers, the elevation was only statistically different after the longest (620-ms duration) pulses that were applied.

Effect of ryanodine on $[Ca^{2+}]_i$ transients elicited by 2-s depolarizing pulses to 0 mV

The above results suggest that, under the present experimental conditions, the effectiveness of ryanodine in affecting intracellular $[Ca^{2+}]$ regulation during depolarization-induced SR calcium release, may strongly depend upon the time during which fibers were transiently depolarized. To underscore this effect clearly, we challenged control and ryanodine-injected fibers with a series of long-duration depolarizing pulses. Fig. 5 illustrates results obtained under such conditions, which actually proved to reveal the most striking effect of ryanodine. Fig. 5 shows two series of indo-1 percentage saturation traces that were obtained in response to 2-s pulses to 0 mV applied every 30 s, in a control fiber (Fig. 5 *A*) and in a ryanodine-injected fiber (Fig. 5 *B*), respectively. To facilitate the comparison, the two sets of traces that are shown were selected for the similar change in dye saturation that was elicited in re-

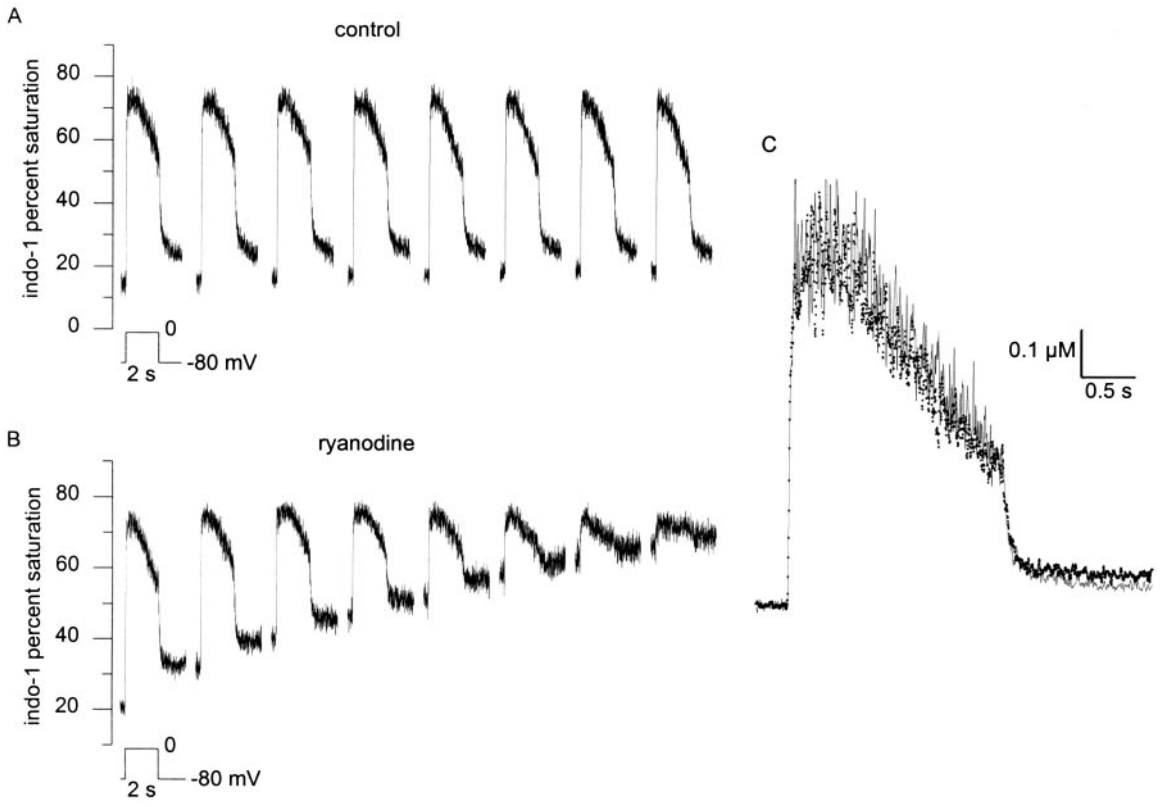

FIGURE 5 $[Ca^{2+}]_i$ signals evoked by 2-s depolarizing pulses to 0 mV in control fibers and in ryanodine-injected fibers. (*A* and *B*), Indo-1 saturation transients elicited by eight successive 2-s depolarizing pulses to 0 mV in a control fiber and in a ryanodine-injected fiber, respectively. A depolarizing pulse was applied every 30 s. (*C*), Enlarged view of the $[Ca^{2+}]_i$ transient calculated from the indo-1 saturation signal elicited by the first depolarization in the control fiber (*continuous line*) and in the ryanodine-injected fiber (*dots*).

sponse to the first depolarization. In the control and in the ryanodine-injected fiber, the first pulse produced a transient change in saturation that yielded an initial rapid decay phase upon repolarization. In the control fiber, this initial decay was followed by a much slower decay phase, only the initial part of which was followed. Within the 30-s period of time that was allowed between two successive pulses, indo-1 saturation had returned to its initial level, indicating a time constant of seconds for the late phase of $[Ca^{2+}]_i$ decay. In the ryanodine-injected fiber, the most remarkable difference was that the final level of dye saturation at the end of the first sampling period remained essentially identical to the baseline level measured 30 s later, just before the second pulse was applied. This suggests that the late phase of $[Ca^{2+}]_i$ decay present in the control fiber was either absent or very much slowed in the ryanodine-injected fiber, leading to a sustained elevated $[Ca^{2+}]_i$ level. Alternatively, it may also be that a slow decay did occur but was followed by a slow rise in $[Ca^{2+}]_i$ within the nonsampled period of time separating the two pulses. This phenomenon re-occurred after each transient, producing in every case a new stepwise increase in resting dye saturation. At the beginning of the eighth transient, dye saturation had reached a value of ~65% corresponding to a $[Ca^{2+}]_i$ level of ~0.6 μM. In Fig. 5 *C*, the change in $[Ca^{2+}]_i$ calculated from the first transient elicited in the control fiber and in the ryanodine-injected fiber, are presented superimposed. It shows that there was hardly any detectable difference between the two transients except during the latest period of time that was sampled.

Fig. 6 shows results from another control fiber and another ryanodine-injected fiber for which indo-1 fluorescence was followed during ~8 s after the end of a 2-s pulse to 0 mV. Fig. 6 *A* shows the dye saturation traces, whereas in Fig. 6 *B*, the low portion of the corresponding $[Ca^{2+}]_i$ traces are presented. The results clearly show the presence of a late, slow phase of $[Ca^{2+}]_i$ decay in the control fiber, but in the ryanodine-injected fiber, the amplitude of this slow component appeared very much reduced. In the control fiber, the $[Ca^{2+}]_i$ value measured at the end of the record corresponded to ~130% of the initial resting $[Ca^{2+}]_i$ measured before the pulse, whereas in the ryanodine-injected fiber, it corresponded to 210% of the initial $[Ca^{2+}]_i$. The solid line superimposed to the decay of the $[Ca^{2+}]_i$ traces corresponds to the result from fitting the sum of two exponential functions plus a constant to the $[Ca^{2+}]_i$ records, starting 10 ms after the end of the depolarization. In both cases, the fit to the decline was satisfactory. In the control fiber and in the ryanodine-injected fiber, the value for the

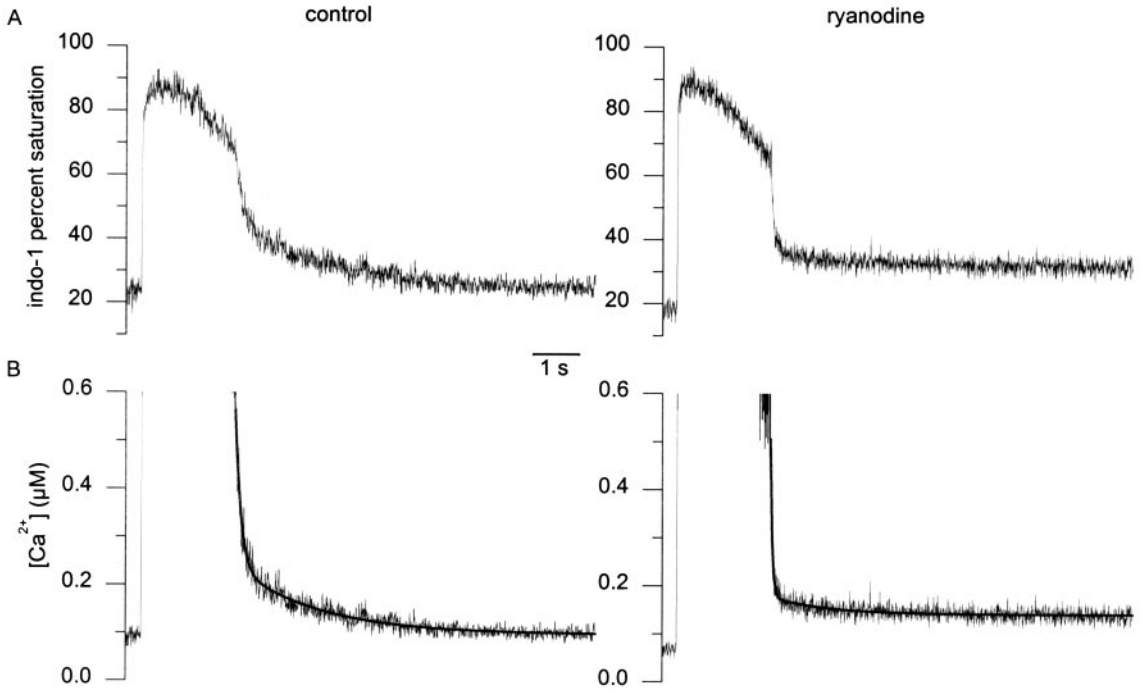

FIGURE 6 Sustained elevated $[Ca^{2+}]_i$ level following a 2-s depolarization to 0 mV in the presence of ryanodine. (*A*), Indo-1 saturation trace from a control fiber (left) and from a ryanodine-injected fiber (right). (*B*), Low portion of the corresponding calculated $[Ca^{2+}]_i$ traces; result from fitting the sum of two exponential functions plus a constant is shown superimposed to the decay of each $[Ca^{2+}]_i$ trace.

slow time constant of $[Ca^{2+}]_i$ decline was 1.7 and 1.2 s, and the corresponding amplitude was 0.14 and 0.035 μM, respectively.

Slope of the use-dependent increase in resting $[Ca^{2+}]_i$ in ryanodine-injected fibers

Fig. 7 *A* shows the time-dependent evolution of the mean resting $[Ca^{2+}]_i$ in control fibers (●) and in ryanodine-injected fibers (○) that were challenged by the same protocol as in Fig. 5. Datapoints for resting $[Ca^{2+}]_i$ were measured as the average baseline value before each depolarizing pulse. Over the full protocol duration, ryanodine-injected fibers exhibited a progressive increase in resting $[Ca^{2+}]_i$ from a mean resting value of 102 ± 14 nM to 443 ± 79 nM ($n = 6$), whereas in the control fibers, resting $[Ca^{2+}]_i$ went from 62 ± 12 nM to 81 ± 11 nM ($n = 8$). It should be noted that in Fig. 7 *A*, the mean initial resting $[Ca^{2+}]_i$ level in the ryanodine-injected fibers was slightly elevated as compared with the control fibers (102 ± 14 nM, $n = 6$ vs. 62 ± 12 nM, $n = 8$, $P = 0.05$). This was attributable to the fact that all ryanodine-injected fibers from this batch had been first depolarized by a series of 20-ms pulses to 0 mV before application of the 2-s pulses. Conversely, for most of corresponding control fibers (7 of 8) no other protocol was applied before the series of 2-s pulses. Comparing the mean initial resting $[Ca^{2+}]_i$ measured at the beginning of the experiment between these two batches of fibers showed no statistical difference (94 ± 14 nM, $n = 6$ ryanodine-injected fibers vs. 62 ± 12 nM, $n = 8$ control fibers, $P = 0.11$). Fig. 7 *B* shows the evolution of resting $[Ca^{2+}]_i$ from experiments similar to the ones described in Fig. 5, the only difference being that the test pulse duration was 0.5 s instead of 2 s. As in Fig. 5 *A*, a progressive rise in free $[Ca^{2+}]_i$ was observed in the ryanodine-injected fibers, although its slope appeared to be less than in the ryanodine-injected fibers tested with 2-s depolarizations. In Fig. 7, *A* and *B*, the straight line superimposed to each series of mean datapoints corresponds to the mean slope calculated from fits of a linear function to datapoints from individual fibers tested under the same condition. In control fibers that were depolarized by 0.5-s and 2-s pulses to 0 mV, the mean value for the slope was −0.4 ± 1 nM ($n = 3$), and 3 ± 1 nM ($n = 8$) per pulse, respectively. In ryanodine-injected fibers that were depolarized by 0.5-s and 2-s pulses to 0 mV, the mean value for the slope was 13 ± 4 nM ($n = 3$) and 48 ± 9 nM ($n = 6$) per pulse, respectively. For a given pulse duration, mean slope values were significantly different between control and ryanodine-injected fibers ($P = 0.03$ for 0.5-s pulses and $P < 0.0001$ for 2-s pulses). In Fig. 5, traces from the ryanodine-injected fiber also indicate that, although there was a profound increase in resting $[Ca^{2+}]_i$, the peak dye saturation remained fairly stable throughout the applied protocol. For fibers to which pulses of 2-s and 0.5-s duration were applied, the mean values for the peak indo-1 saturation are plotted in Fig. 7, *C* and *D*, respectively. The peak saturation

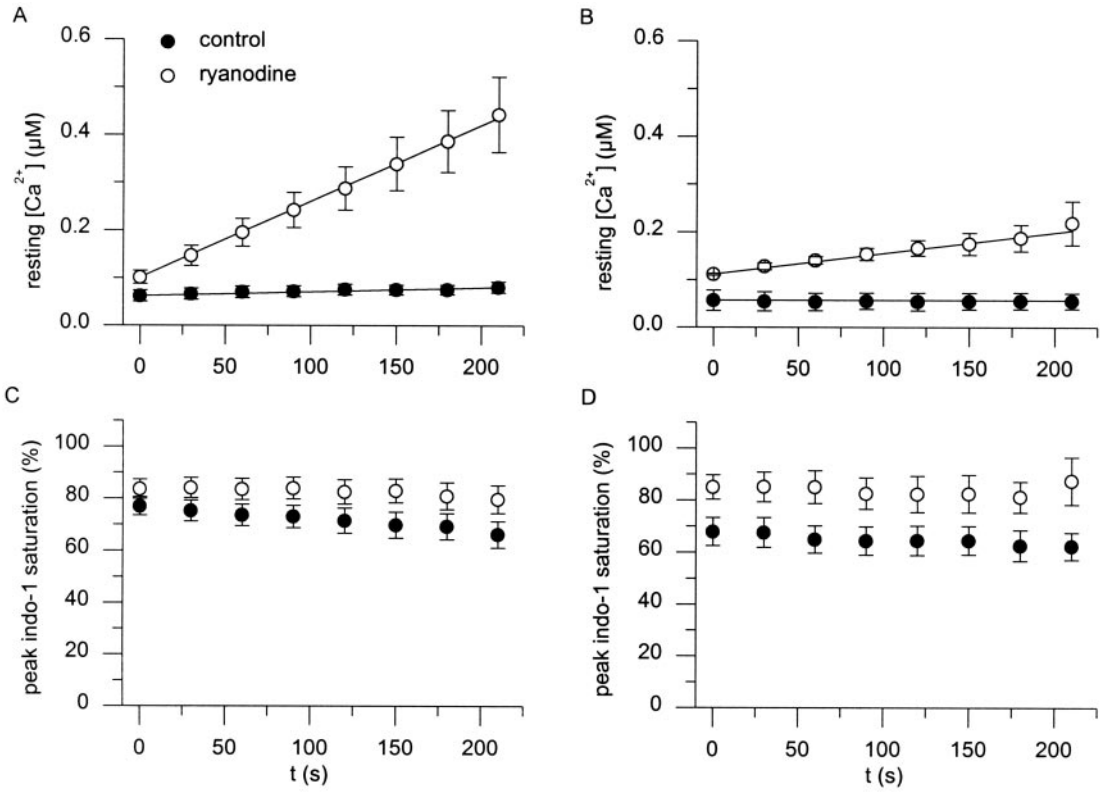

FIGURE 7 (*A*), Time-dependent evolution of the mean ± SE value for resting $[Ca^{2+}]_i$ in control fibers (●, $n = 8$) and in ryanodine-injected fibers (○, $n = 6$) over the course of experiments during which a 2-s pulse to 0 mV was applied every 30 s. (*B*), Same as in *A*, except that the pulse duration was 0.5 s (data are from 3 control fibers and 3 ryanodine-injected fibers). (*C*), Evolution of the mean ± SE value for the peak indo-1 saturation level measured during the pulse, in control fibers and in ryanodine-injected fibers that were stimulated by a 2-s pulse to 0 mV applied every 30 s (same fibers as in *A*). (*D*), same as in *C*, except that the pulse duration was 0.5 s (same fibers as in *B*). In *A* and *B*, the straight lines superimposed to the datapoints correspond to the mean slope of change in resting $[Ca^{2+}]_i$ from fits of a linear function to datapoints from individual fibers (see text for details).

was tabulated rather than the actual peak $[Ca^{2+}]_i$, because the high levels of saturation reached in some fibers rendered an accurate estimation of free calcium concentration quite difficult. In any case, results show that the increase in resting $[Ca^{2+}]_i$ observed in the ryanodine-injected fibers was not accompanied by a simultaneous parallel evolution of the peak $[Ca^{2+}]_i$ level reached during the pulses. Results from this overall series of experiments show that the presence of ryanodine within the cytoplasm clearly affected intracellular $[Ca^{2+}]$ regulation during the E-C coupling process, and this in a use-dependent manner. The sustained $[Ca^{2+}]_i$ level most clearly observed after long-lasting depolarizing pulses can be intuitively related to the reported "open-lock" effect of ryanodine at the single ryanodine receptor channel level. Assuming that ryanodine binds to ryanodine receptor channels that open upon membrane depolarization and that ryanodine-bound channels are no longer sensitive to membrane voltage, one is to expect an increased sustained SR Ca^{2+} leak to follow membrane repolarization. The following section aims at assessing the potential effects of such a mechanism using $[Ca^{2+}]_i$ transients simulated on the basis of simple intracellular calcium distribution models of skeletal muscle.

Simulation of the effects of an increased SR Ca^{2+} leak consecutive to membrane repolarization on the $[Ca^{2+}]_i$ transients

Fig. 8 shows results from simulations that used a simple model of intracellular calcium distribution to derive the time course of change in $[Ca^{2+}]_i$ from a synthetic release rate record (see Methods). In Fig. 8, all four panels show, from top to bottom, synthetic Ca^{2+} release-rate traces, calcium bound to the slow buffer (CaS), uptake of Ca^{2+} into the nonsaturable compartment and $[Ca^{2+}]_i$. In each case, transient increases in release rate of various duration were used to simulate the effect of membrane depolarizations of various duration. Fig. 8, *A* and *C* show results from a "control simulation"; the transient changes in release rate were made to return to the initial resting level. In the "ryanodine simulation" (Fig. 8, *B* and *D*) the transient changes in release rate were made to return to an identical constant value that was larger than the initial resting level (increased Ca^{2+} leak). Fig. 8, *C* and *D* show the same simulations as Fig. 8, *A* and *B*, respectively, but over a longer period of time, and also including an additional simulation using a 1-s transient change in release rate. Overall results show that a

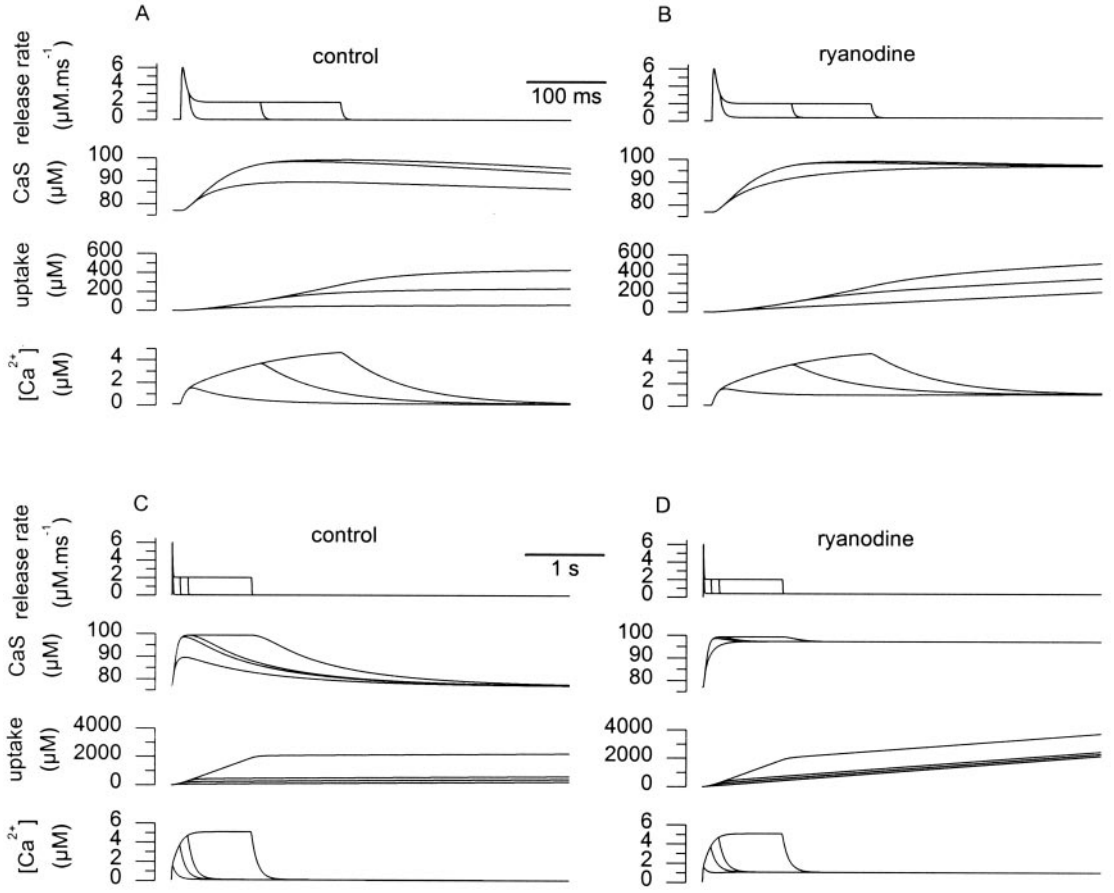

FIGURE 8 Simulation of the effects of a depolarization-induced SR Ca^{2+} leak using a simple model of intracellular Ca^{2+} distribution. In *A–D*, series of traces shown from top to bottom, correspond to 1) synthetic Ca^{2+} release rate traces simulating release evoked by depolarizations of various duration (10, 100, and 200 ms); 2) corresponding time course of calcium bound to the slow buffer (CaS); 3) corresponding uptake of Ca^{2+} into the nonsaturable compartment (uptake); and 4) corresponding changes in $[Ca^{2+}]_i$. In *A* and *C*, release rates were made to rapidly return to the initial level following the end of the transient change (control simulation). In *B* and *D*, transient changes in release rates was made to return to a constant elevated value as compared with the initial level (ryanodine simulation). *C* and *D* show the same simulations as *A* and *B*, respectively, but over a longer period of time. Furthermore, *C* and *D* include results from an additional simulation using a longer duration (1 s) change in release rate. See Methods section and text for details.

chronically increased Ca^{2+} leak, occurring as the consequence of a transient membrane depolarization, can qualitatively account for the postpulse $[Ca^{2+}]_i$ elevation observed in the presence of ryanodine. In the ryanodine simulation, $[Ca^{2+}]_i$ transients still exhibit an early, sharp decay after the end of the transient change in release. However, as a consequence of the increased Ca^{2+} leak, the calcium occupancy of the slow buffer and the free calcium remain elevated, whereas the uptake system keeps operating at an increased rate, as compared with the control conditions. Fig. 9 shows results from another set of simulations that fit with the use-dependence of the ryanodine effect; for this, the amplitude of the Ca^{2+} leak that followed a given depolarization was made to be proportional to the duration of the depolarization. In Fig. 9, all panels show the results from the same simulations but with different levels of either *x* or *y* axis magnification. Also, in Fig. 9, *C* and *D*, an additional release trace simulating the effect of a 1-s depolarization was included. For simplicity only the release rate and $[Ca^{2+}]_i$ traces are shown. Under such conditions, the longer the depolarization, the higher the amplitude of the postpulse elevation in $[Ca^{2+}]_i$. Qualitatively identical results were obtained with a more elaborated model (see Methods) that took into account the main properties of intracellular calcium buffering and uptake in skeletal muscle (not illustrated).

Effect of ryanodine for various levels of step membrane depolarization

The preceding results and simulations are consistent with the possibility that ryanodine binds to release channels that open during membrane depolarization, and that increasing the duration of depolarization increases the number of ryanodine-bound release channels. An alternative way to test

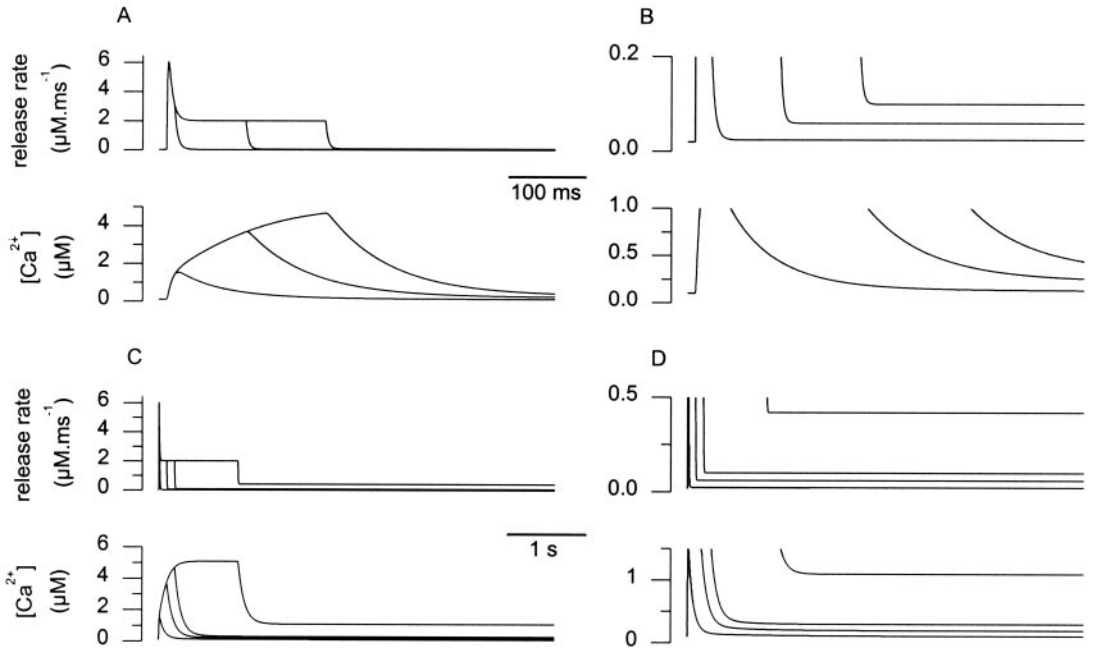

FIGURE 9 Simulation of the effects of a depolarization-induced SR Ca^{2+} leak assuming the amplitude of the leak to increase with the pulse duration. Simulations were performed with the same model as used in Fig. 8. (*A—D*), synthetic Ca^{2+} release traces (*top traces*) simulating release evoked by depolarizations of increasing duration and corresponding calculated time course of change in $[Ca^{2+}]_i$ (*bottom traces*). In all cases, the transient changes in release rate were made to return to a constant elevated value (as compared with the initial level); the amplitude of this elevated level was made to increase linearly with the pulse duration. (*C* and *D*), same simulations as in *A* and *B*, but over a longer period of time and also including result from an additional simulation using a longer duration (1 s) transient change in release rate. (*B* and *D*), lower expanded portion of the traces shown in *A* and *C*, respectively. See Methods section and text for details.

for such a possibility was to study the effect of ryanodine under various levels of membrane depolarization, which represents another way of potentially recruiting a variable fraction of release channels.

Fig. 10 *B* shows indo-1 percentage saturation traces elicited by 12 successive 2-s duration depolarizing pulses to −30 mV followed by 12 pulses of same duration to −10 mV. Pulses of same amplitude were applied every 30 s, and a 1 min delay was allowed at the time when the pulse amplitude was increased. Fig. 10 *C* shows the corresponding time-dependent evolution of the resting $[Ca^{2+}]_i$ level during the course of the experiment. It shows that the slope of resting $[Ca^{2+}]_i$ increase was larger during the series of pulses to −10 mV than during the series of lower amplitude ones. The two straight lines superimposed to the datapoints correspond to a slope of 4 nM per pulse and 33 nM per pulse for depolarizations to −30 and −10 mV, respectively. Qualitatively similar results were obtained in three additional fibers that took series of 2-s duration pulses to −20 mV and 0 mV, giving a mean slope of increase in resting $[Ca^{2+}]_i$ of 10 ± 5 nM per pulse and 42 ± 3 nM per pulse, respectively.

Assuming that the increase in resting $[Ca^{2+}]_i$ brought by a depolarization of given amplitude is proportional to the increase in SR calcium leak, a simple, straightforward explanation for the above effect would be that, within the voltage-sensitive range of calcium release, raising the amplitude of the depolarization opens up an increased fraction of release channels during the pulse. As a consequence, an increased number of channels would potentially bind ryanodine and remain locked in a partially open state after repolarization. However, this interpretation should also take into account the fact that, opening a larger fraction of release channels also produces an increased peak $[Ca^{2+}]_i$ level during the pulse which, by itself, may be expected to potentiate ryanodine binding. In an attempt to explore the occurrence of such an effect, we examined the dependence of the postpulse elevation in resting $[Ca^{2+}]_i$ upon the maximal amplitude of the free $[Ca^{2+}]_i$ reached during the pulse, and this for fibers that were transiently depolarized to the same level.

Dependence of the amplitude of the rise in resting $[Ca^{2+}]_i$ consecutive to a depolarization upon the peak $[Ca^{2+}]$ reached during the pulse

Fig. 11 shows the dependence of the amplitude of the change in resting $[Ca^{2+}]$ ($\Delta[Ca^{2+}]_{rest}$) produced by a 2-s depolarization to 0 mV, versus the peak $[Ca^{2+}]_i$ reached during the pulse, in control fibers (●) and in ryanodine-injected fibers (○). It was obtained by pooling all data from

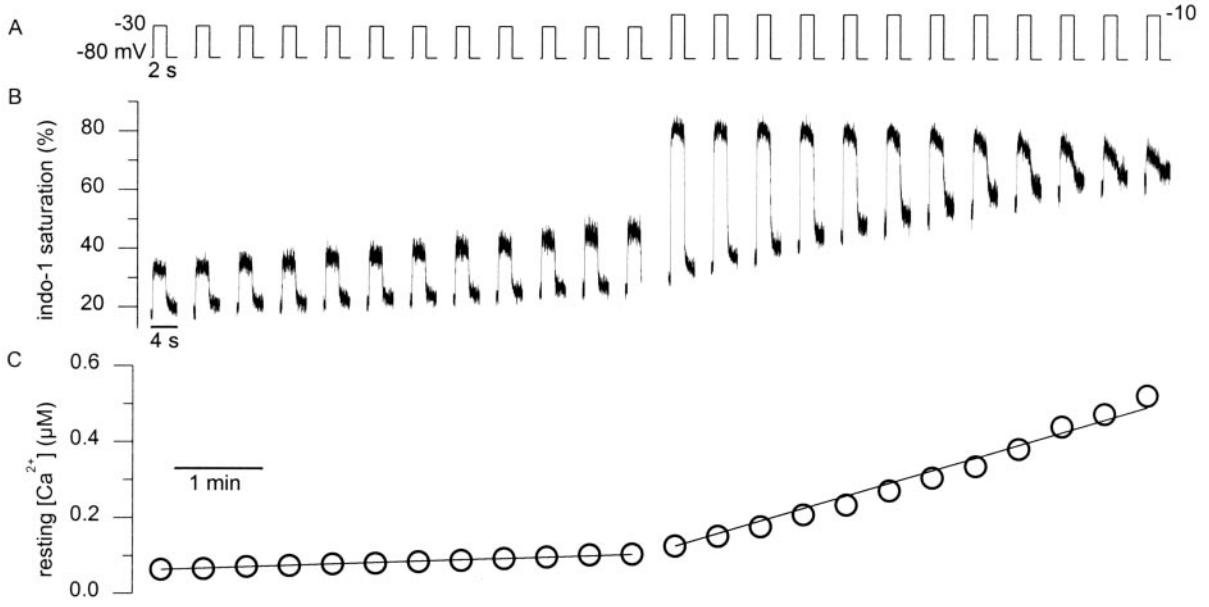

FIGURE 10 Dependence of the ryanodine-induced increase in resting $[Ca^{2+}]_i$ upon the amplitude of the depolarizing pulse. (*A*), Pulse protocol: 2-s depolarizing pulses to −30 mV were followed by 12 pulses to −10 mV of the same duration. Pulses of same amplitude were applied every 30 s. (*B*), Indo-1 saturation traces elicited by the protocol shown in *A*. (*C*), Time course of the change in resting $[Ca^{2+}]_i$ over the course of the experiment. The two straight lines superimposed to the datapoints correspond to the result of a linear fit.

fibers that were challenged by the protocol illustrated in Fig. 5: values for $\Delta[Ca^{2+}]_{rest}$ were obtained by subtracting the $[Ca^{2+}]_i$ level measured before a depolarization, to the value measured 30 s later, just before the next depolarization was applied. Data were then sorted according to the peak $[Ca^{2+}]_i$ reached during the pulse, and the $\Delta[Ca^{2+}]_{rest}$ values falling within the same range of corresponding peak $[Ca^{2+}]_i$ (with an increment arbitrarily set to 0.4 μM) were averaged. For peak $[Ca^{2+}]$ values higher than 2 μM, all corresponding data were averaged. It should be mentioned that the variability of the peak $[Ca^{2+}]_i$ values which is being taken advantage of here, results essentially from fiber to fiber variability, and that a similar figure would be obtained if one were to plot the individual mean values of $\Delta[Ca^{2+}]_{rest}$ versus mean peak $[Ca^{2+}]_i$ for each fiber (not illustrated). In any case, results show that, in ryanodine-injected fibers, the amplitude of the rise in resting $[Ca^{2+}]_i$ produced by a same depolarization seems to depend upon the peak $[Ca^{2+}]_i$ reached during the pulse. Although in Fig. 11 it was tempting to fit the ryanodine datapoints with an Hill equation, uncertainty concerning the highest $[Ca^{2+}]_i$ levels along the *x* axis, because of heavy saturation of the indicator, would make the fit results doubtful.

Effect of injecting a high ryanodine concentration on $[Ca^{2+}]_i$ transients

In another series of experiments we attempted to test the effect of a higher intracellular ryanodine concentration than in the previously described experiments. For this, the dye injecting pipette contained 0.8 mM instead of 0.1 mM ryanodine (see Methods). These conditions were found to be quite extreme as 70% of the injected fibers died during the period of dye (and ryanodine) equilibration, and only in a few fibers were we able to record $[Ca^{2+}]_i$ transients elicited by membrane depolarizations. Fig. 12 *A* shows indo-1 saturation transients measured from one of these fibers, to which the protocol shown in Fig. 4 was applied. Traces shown from top to bottom of Fig. 12 *A* correspond to the transients elicited by four successive 20-ms membrane depolarizations to 0 mV, followed by four 220-ms pulses to the same potential. Results show that a postpulse steady elevation of dye saturation could already be detected after each of the successive 20-ms pulses, corresponding to an increase in $[Ca^{2+}]_i$ to ~80, 90, 95, and 110 nM, from the initial resting level of ~65 nM, respectively. Most spectacular was the result from the following first 220-ms pulse which produced a very substantial postpulse increase in dye saturation, corresponding to a $[Ca^{2+}]_i$ elevation from a prepulse level of 110 nM to 215 nM. The effect was again present in response to the next 220-ms depolarizations, which brought the dye saturation to corresponding $[Ca^{2+}]_i$ levels of 265 nM and 345 nM, respectively. In Fig. 12 *B* the open triangles correspond to the mean change in resting $[Ca^{2+}]_i$ measured from three fibers injected with the 0.8-mM ryanodine-containing solution, versus the period of time along which that same protocol was applied. For comparison, data obtained from control fibers and from fibers that were injected with the 0.1 mM ryanodine containing solution (same data as in Fig. 4 *D*) are shown on the same

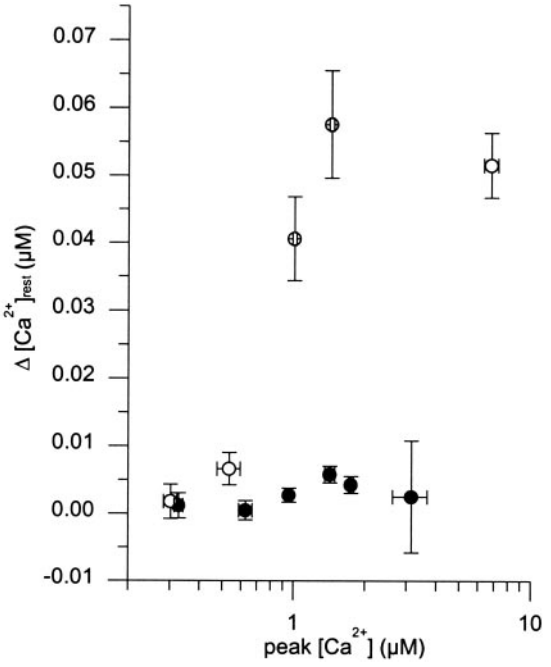

FIGURE 11 Dependence of the change in resting free calcium ($\Delta[Ca^{2+}]_{rest}$) produced by a 2-s depolarization to 0 mV upon the peak $[Ca^{2+}]_i$ reached during the pulse. Data are from control fibers (●) and ryanodine-injected fibers (○) that took a series of 2-s depolarizations to 0 mV (same protocol as in Fig. 5). $\Delta[Ca^{2+}]_{rest}$ values were obtained by subtracting the $[Ca^{2+}]_i$ level measured before a given pulse to the level measured 30 s later, just before the next pulse was applied. Mean (± SE) $\Delta[Ca^{2+}]_{rest}$ values were obtained by averaging data that fell within a similar range of corresponding peak $[Ca^{2+}]_i$ levels (measured during the pulse).

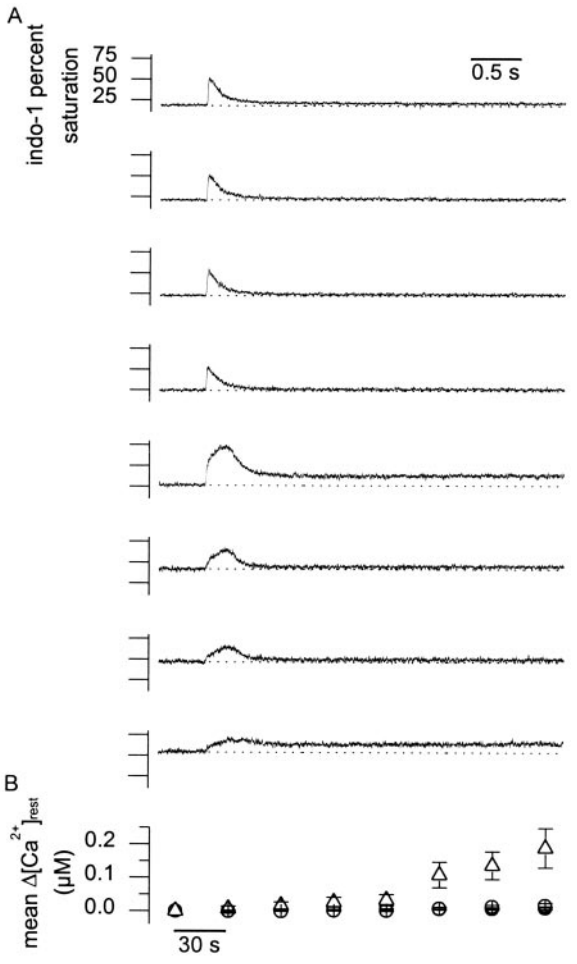

FIGURE 12 Effect of injecting a high intracellular concentration of ryanodine. (*A*), Indo-1 saturation traces elicited by (from top to bottom) successive depolarizations to 0 mV: four pulses of 20-ms duration were followed by four pulses of 220-ms duration. Dotted lines correspond to the initial saturation level of each trace. Data are from a fiber that was injected with a 0.8-mM ryanodine-containing solution, expected to produce a final intracellular ryanodine concentration within an ~50–100 μM range. (*B*), Time course of mean change in resting $[Ca^{2+}]_i$ over the course of the protocol shown in *A*, in control fibers (●, $n = 5$), in fibers that were injected with the 0.1-mM ryanodine-containing solution (○, $n = 4$), and in fibers that were injected with the 0.8-mM ryanodine-containing solution (△, $n = 3$).

graph (● and ○, respectively). Results clearly show that, for a given depolarization, the relative elevation in postpulse $[Ca^{2+}]_i$ increased with the ryanodine concentration.

DISCUSSION

The present results provide new insights into the mechanism of modulation of the E-C coupling process by ryanodine. In addition, they emphasize the physiological relevance of some of the most classically described effects of ryanodine on its isolated receptor. From a more general point of view, our results also prove the present experimental conditions, consisting in measuring intracellular $[Ca^{2+}]$ under membrane voltage control in a fiber previously injected with a pharmacological tool, to be reliable when studying the regulation of SR calcium release in a functioning muscle fiber.

Ryanodine has been extensively used on various types of skeletal muscle preparations, providing breakthrough insights into the details of its mechanism of action, and most interestingly, into the operating and regulation of the SR release channels (Coronado et al., 1994; Meissner, 1994; Franzini-Armstrong and Protasi, 1997; Sutko et al., 1997). However, although the effects of ryanodine have been particularly well studied on isolated release channels, SR vesicles preparations, skinned fibers, and in intact muscle, the as-yet published results concerning its effects on intracellular calcium in a skeletal muscle fiber under voltage control do not fully account for what may be expected from the effects reported on more fragmented preparations. Mainly, in frog fibers, ryanodine (1–100 μM) was shown to initially potentiate the intracellular calcium transient elicited by a voltage-clamp depolarization, and to then cause a slowly developing inhibitory effect (Garcia et al., 1991). Our results in mouse skeletal muscle fibers demonstrate that the most prevailing effect of micromolar levels of ryanodine is

to induce a chronic elevation of the resting $[Ca^{2+}]_i$ level that requires membrane depolarization to occur. Although we could not accurately estimate the ryanodine concentration within the injected fibers, this effect seemed to be dose dependent as it could be more readily detected under injection conditions expected to produce an ~10 times higher concentration of ryanodine in the fiber. We believe it is attributable to ryanodine binding to open release channels, and having the same functional consequences that were described at the isolated ryanodine receptor level. Under control conditions, membrane depolarization opens release channels, producing a rise in intracellular free calcium concentration. While depolarization is maintained, the overall time course of change in $[Ca^{2+}]_i$ is a complex function depending on the amplitude and waveform of the calcium release rate and of the rate of Ca^{2+} removal from the cytosolic compartment through the effect of high- and low-affinity intrinsic calcium buffers and SR calcium pumping. Upon repolarization, as release turns off, $[Ca^{2+}]_i$ decays back toward its initial resting level because of the sole action of the removal mechanisms. When depolarizing in the presence of ryanodine, opening of release channels as well as the consecutive increase in myoplasmic $[Ca^{2+}]$ are both expected to favor binding of the alkaloid, which should then leave the channels in a partially open substate (Meissner, 1986; Pessah et al., 1987). Under our conditions, in the presence of ryanodine, the time course of the $[Ca^{2+}]_i$ transient during the pulse looked similar to what was observed in control fibers. In addition, $[Ca^{2+}]_i$ transients also exhibited a rapid decaying phase after repolarization, indicating that a substantial fraction of the release channels that opened during the pulse did turn off after its end. Again, the most remarkable effect of ryanodine was the close to steady increased $[Ca^{2+}]_i$ level that was observed following sufficiently long depolarizing pulses. Under normal conditions, the resting $[Ca^{2+}]_i$ level is to result from a balance between a constant SR Ca^{2+} leak and SR Ca^{2+} pumping. An increased resting level is thus to reflect either a reduced Ca^{2+} pumping rate, or an increased SR Ca^{2+} leak. As the time course of $[Ca^{2+}]_i$ decay after short pulses was found to be even faster in the presence of ryanodine than in control fibers, it is very unlikely that the SR pumping rate was reduced in the presence of ryanodine. Also, an effect of ryanodine on SR ATP-dependent calcium transport is unlikely as calcium influx into longitudinal SR membranes was previously shown to be unaffected by the alkaloid (Lattanzio et al., 1987). Along this line, it may be worth mentioning that, although we have no straightforward explanation for the faster relaxation rate, this effect is consistent with the initial acceleration of twitch relaxation produced by 1 μM of the alkaloid in rat skeletal muscle fibers (Fryer et al., 1989). As also supported by the results from the simulations, this leaves an increased SR calcium leak as the most prevailing explanation for the chronically elevated $[Ca^{2+}]_i$ level that was observed following sufficiently long depolarizing pulses. This interpretation is consistent with the single channel data showing that ryanodine permanently opens the release channels into a subconductance state (Imagawa et al., 1987; Rousseau et al., 1987). It is also consistent with results from skinned fibers (Lamb and Stephenson, 1990) showing that depolarization-induced contraction was prolonged in the presence of ryanodine, and could not be stopped upon repolarization. Accordingly, our results also suggest that, in an intact muscle fiber, ryanodine-bound channels are no longer under the control of the voltage sensor, or at least that some of them fail to turn off after membrane repolarization. In contrast with the results from Lamb and Stephenson (1990) showing that after a depolarization in the presence of 25 μM ryanodine, no subsequent depolarization could elicit a response, we could not find any clear evidence, from the presently tested experimental conditions, for ryanodine having a blocking shut effect on the release activity. Specific differences between the two preparations and experimental conditions may be responsible for this discrepancy. It could also be speculated that, under the skinned fiber conditions used by Lamb and Stephenson (1990), depolarization activated the majority of the release channels, and that it would not be the case, for instance under our conditions of 2-s depolarization to 0 mV.

Apart from giving credit to the physiological relevance of the open-lock effect of ryanodine, our results also put forward interesting issues concerning the calcium release activity during a voltage-clamp pulse.

A point which is of specific interest is the $[Ca^{2+}]$ dependence of the phenomenon. The activity of the SR release channels as well as the binding of ryanodine are promoted by micromolar levels of Ca^{2+} (Pessah et al., 1987; Smith et al., 1988; Meissner and el-Hashem, 1992). In the skinned fiber preparation, ryanodine was also found to be ineffective when $[Ca^{2+}]$ was buffered at very low levels (Lamb and Stephenson, 1990), and it is generally believed that the Ca^{2+}-dependence of ryanodine binding is attributable to release channels being opened by Ca^{2+} rather than on an effect of Ca^{2+} on ryanodine binding. Under our conditions, we found that the effectiveness of ryanodine in producing a sustained increase in $[Ca^{2+}]_i$ following a given depolarization seemed to depend on the peak $[Ca^{2+}]_i$ reached during the pulse. Interpretation of these data should though be taken with caution as a high-peak $[Ca^{2+}]_i$ could simply be related to a high level of release channels being open, and thus to a large fraction of channels being given access to ryanodine binding.

A postpulse elevation in $[Ca^{2+}]_i$ observed in the presence of ryanodine could be reproduced after successive depolarizations in a same fiber, leading to a quasilinear relationship between resting $[Ca^{2+}]_i$ and time, as the pulses were applied at constant frequency. This is consistent with an additional, probably similar fraction of release channels being bound to ryanodine during each successive pulse. The slope of rise in resting $[Ca^{2+}]_i$ seemed to depend not only upon the ryanodine con-

centration but also on the duration of the depolarizing pulse, suggesting that an increasing number of release channels gets activated as the pulse duration is increased. Along this line, the fact that we could hardly detect the effect of ryanodine when short (20-ms long) pulses were used can be taken as evidence that only a restricted fraction of release channels activate under such pulse protocol.

Finally, it should be stressed that the overall details of how ryanodine affects SR calcium regulation in an intact fiber are certainly more complex than inferred from above. For instance, it is far from easy to speculate about how processes such as voltage-dependent inactivation of the voltage sensors, Ca^{2+}-dependent inactivation of release channels, SR Ca^{2+} depletion, retrograde signaling between release channels and voltage sensors (Gonzalez and Caputo, 1996) would modulate the overall effect of ryanodine and/or be affected in the presence of the alkaloid. Also, it is not clear whether or not ryanodine-bound, open-locked release channels are still sensitive to activation by Ca^{2+} as there seems to be conflicting results between single channel data (Rousseau et al., 1987) and skinned fibers data (Oyamada et al., 1993).

In conclusion, although a complete understanding of the effects of ryanodine on E-C coupling will require additional efforts, our results provide original clues to how the alkaloid affects intracellular calcium regulation in an intact skeletal muscle fiber. In addition, they demonstrate the efficiency of the presently used experimental approach for giving insights into the physiological regulation of SR calcium release.

We thank Drs B. Allard, C. Ojeda, and O. Rougier for helpful discussion and comments on the manuscript. This study was supported by the Center National de la Recherche Scientifique (CNRS) and the University Claude Bernard.

REFERENCES

Baylor, S. M., W. K. Chandler, and M. W. Marshall. 1983. Sarcoplasmic reticulum calcium release in frog skeletal muscle fibres estimated from Arsenazo III calcium transients. *J. Physiol.* 344:625–666.

Brum, G., E. Rios, and E. Stefani. 1988. Effects of extracellular calcium on calcium movements of excitation-contraction coupling in frog skeletal muscle fibres. *J. Physiol.* 398:441–473.

Buck, E., I. Zimanyi, J. J. Abramson, and I. N. Pessah. 1992. Ryanodine stabilizes multiple conformational states of the skeletal muscle calcium release channel. *J. Biol. Chem.* 267:23560–23567.

Bull, R., J. J. Marengo, B. A. Suarez-Isla, P. Donoso, J. L. Sutko, and C. Hidalgo. 1989. Activation of calcium channels in sarcoplasmic reticulum from frog muscle by nanomolar concentrations of ryanodine. *Biophys. J.* 56:749–756.

Collet, C., B. Allard, Y. Tourneur, and V. Jacquemond. 1999. Intracellular calcium signals measured with indo-1 in isolated skeletal muscle fibres from control and *mdx* mice. *J. Physiol.* 520:417–429.

Coronado, R., J. Morrissette, M. Sukhareva, and D. M. Vaughan. 1994. Structure and function of ryanodine receptors. *Am. J. Physiol.* 266: C1485–C1504.

Csernoch, L., J. C. Bernengo, P. Szentesi, and V. Jacquemond. 1998. Measurements of intracellular Mg^{2+} concentration in mouse skeletal muscle fibers with the fluorescent indicator mag-indo-1. *Biophys. J.* 75:957–967.

Franzini-Armstrong, C., and F. Protasi. 1997. Ryanodine receptors of striated muscles: a complex channel capable of multiple interactions. *Physiol. Rev.* 77:699–729.

Fryer, M. W., G. D. Lamb, and I. R. Neering. 1989. The action of ryanodine on rat fast and slow intact skeletal muscles. *J. Physiol.* 414:399–413.

Garcia, J., A. J. Avila-Sakar, and E. Stefani. 1991. Differential effects of ryanodine and tetracaine on charge movement and calcium transients in frog skeletal muscle. *J. Physiol.* 440:403–417.

Garcia, J., and M. F. Schneider. 1993. Calcium transients and calcium release in rat fast-twitch skeletal muscle fibres. *J. Physiol.* 463:709–728.

Gonzalez, A., and C. Caputo. 1996. Ryanodine interferes with charge movement repriming in amphibian skeletal muscle fibers. *Biophys. J.* 70:376–382.

Gonzalez, A., W. G. Kirsch, N. Shirokova, G. Pizarro, G. Brum, I. N. Pessah, M. D. Stern, H. Cheng, and E. Rios. 2000. Involvement of multiple intracellular release channels in calcium sparks of skeletal muscle. *Proc. Natl. Acad. Sci. U.S.A.* 97:4380–4385.

Imagawa, T., J. S. Smith, R. Coronado, and K. P. Campbell. 1987. Purified ryanodine receptor from skeletal muscle sarcoplasmic reticulum is the Ca^{2+}-permeable pore of the calcium release channel. *J. Biol. Chem.* 262:16636–16643.

Jacquemond, V. 1997. Indo-1 fluorescence signals elicited by membrane depolarization in enzymatically isolated mouse skeletal muscle fibers. *Biophys. J.* 73:920–928.

Lamb, G. D., and D. G. Stephenson. 1990. Control of calcium release and the effect of ryanodine in skinned muscle fibres of the toad. *J. Physiol.* 423:519–542.

Lattanzio, F. A., R. G. Schlatterer, M. Nicar, K. P. Campbell, and J. L. Sutko. 1987. The effects of ryanodine on passive calcium fluxes across sarcoplasmic reticulum membranes. *J. Biol. Chem.* 262:2711–2718.

Meissner, G. 1986. Ryanodine activation and inhibition of the Ca^{2+} release channel of sarcoplasmic reticulum. *J. Biol. Chem.* 261:6300–6306.

Meissner, G. 1994. Ryanodine receptor/Ca^{2+} release channels and their regulation by endogenous effectors. *Annu. Rev. Physiol.* 56:485–508.

Meissner, G., and A. El-Hashem. 1992. Ryanodine as a functional probe of the skeletal muscle sarcoplasmic reticulum Ca^{2+} release channel. *Mol. Cell. Biochem.* 114:119–123.

Oyamada, H., M. Iino, and M. Endo. 1993. Effects of ryanodine on the properties of Ca^{2+} release from the sarcoplasmic reticulum in skinned skeletal muscle fibres of the frog. *J. Physiol.* 470:335–348.

Pessah, I. N., R. A. Stambuk, and J. E. Casida. 1987. Ca^{2+}-activated ryanodine binding: mechanisms of sensitivity and intensity modulation by Mg^{2+}, caffeine, and adenine nucleotides. *Mol. Pharmacol.* 31: 232–238.

Rios, E., and G. Pizarro. 1991. Voltage sensor of excitation-contraction coupling in skeletal muscle. *Physiol. Rev.* 71:849–908.

Rousseau, E., J. S. Smith, and G. Meissner. 1987. Ryanodine modifies conductance and gating behavior of single Ca^{2+} release channel. *Am. J. Physiol.* 253:C364–C368.

Shirokova, N., J. Garcia, G. Pizarro, and E. Rios. 1996. Ca^{2+} release from the sarcoplasmic reticulum compared in amphibian and mammalian skeletal muscle. *J. Gen. Physiol.* 107:1–18.

Smith, J. S., T. Imagawa, J. Ma, M. Fill, K. P. Campbell, and R. Coronado. 1988. Purified ryanodine receptor from rabbit skeletal muscle is the calcium-release channel of sarcoplasmic reticulum. *J. Gen. Physiol.* 92:1–26.

Su, J. Y. 1987. Effects of ryanodine on skinned skeletal muscle fibers of the rabbit. *Pflügers Arch.* 410:510–516.

Sutko, J. L., J. A. Airey, W. Welch, and L. Ruest. 1997. The pharmacology of ryanodine and related compounds. *Pharmacol. Rev.* 49:53–98.

Szentesi, P., V. Jacquemond, L. Kovacs, and L. Csernoch. 1997. Intramembrane charge movement and sarcoplasmic calcium release in enzymatically isolated mammalian skeletal muscle fibres. *J. Physiol.* 505: 371–384.

Timmer, J., T. Muller, and W. Melzer. 1998. Numerical methods to determine calcium release flux from calcium transients in muscle cells. *Biophys. J.* 74:1694–1707.